Journal of Alloys and Compounds 579 (2013) 249–252

Contents lists available at SciVerse ScienceDirect

Journal of Alloys and Compounds

journal homepage: www.elsevier.com/locate/jalcom

Characteristics of the stress-induced formation of R-phase in ultrafine-grained NiTi shape memory wire

J. Olbricht [a,b,*], A. Yawny [c,d], J.L. Pelegrina [c,d], G. Eggeler [a], V.A. Yardley [a]

[a] Institute for Materials, Ruhr University Bochum, 44780 Bochum, Germany
[b] BAM Federal Institute for Materials Research and Testing, 12200 Berlin, Germany
[c] Centro Atómico Bariloche, 8400 San Carlos de Bariloche, Argentina
[d] Instituto Balseiro and CONICET, Argentina

ARTICLE INFO

Article history:
Received 12 March 2013
Received in revised form 23 May 2013
Accepted 10 June 2013
Available online 18 June 2013

Keywords:
NiTi shape memory alloys
Pseudoelasticity
Stress-induced phase transformations
Localization
R-phase

ABSTRACT

The transformation between the cubic B2 and monoclinic B19′ phases in ultrafine-grained pseudoelastic NiTi can occur as a two-step process involving the intermediate rhombohedral R-phase. Experimental work using differential scanning calorimetry, electrical resistance measurements and transmission electron microscopy has demonstrated the formation of this intermediate phase during thermal cycling and during mechanical loading. In the present paper, complementary mechanical and thermographic results are presented which allow to further assess the character of the stress-induced R-phase formation. The transformation from B2 to R-phase is demonstrated to occur homogeneously within the gauge length rather than via advancing Lüders-type transition regions as it is the case in the localized transformation from B2 or R-phase to B19′.

1. Introduction

Near-equiatomic binary NiTi shape memory alloys are of great technological interest because of their good structural and functional properties [1,2] and their range of possible biomedical and engineering applications [3,4]. Commercial NiTi wires and tubes typically exhibit ultrafine-grained microstructures which provide high resistance to plastic deformation, thus favoring the reversible martensitic transformation necessary for pseudoelasticity. The transformation from the high-temperature B2 cubic "austenite" phase [2,5] to the low-temperature monoclinic B19′ "martensite" phase [6,7] may occur via an intermediate rhombohedral structure referred to as "R-phase" [8]. The lattice correspondences between these three phases have been established in [9–12].

Differential scanning calorimetry (DSC) and electrical resistance measurements reported in [13] using both partial and full thermal cycles support the view that the transformation between B2 and B19′ in commercial pseudoelastic NiTi wires (nominal composition 50.9 at.% Ni) on heating and cooling without an applied load does occur via an intermediate transformation to R-phase. Transmission electron microscopy (TEM) using in-situ cooling confirmed load-free thermally induced formation of R-phase at −20 °C by the appearance of diffraction reflections corresponding to its crystal structure [13].

The stress-induced formation of the R-phase at constant temperature has been investigated in a NiTiFe alloy [14] and in binary NiTi [15]. In both systems, two-stage yielding phenomena associated with the separate R-phase and B19′ martensite transitions were observed. Optical microscopic observations have demonstrated that the R-phase exhibits all features typical of a martensitic microstructure: It has four variants that accommodate one another, it shows the one way shape memory effect and on application of a mechanical stress, the favorably oriented variants grow at the expense of the others [16]. During TEM in-situ straining experiments performed in Ni rich 50.9 wt% NiTi pseudoelastic wires, the formation of B19′ was observed but some of the emerging diffraction reflections could only be accounted for by considering the additional presence of the R-phase [13]. This is direct evidence of stress-induced R-phase formation. Šittner et al. used in-situ neutron diffraction and ultrasonic experiments to investigate the transformation between B2 and R-phase and the reorientation of R-phase during loading [17]. They concluded that these methods and also variations in electrical resistance are more sensitive than mechanical methods for the characterization of transformations which involve the R-phase [18].

* Corresponding author at: BAM Federal Institute for Materials Research and Testing, 12200 Berlin, Germany. Tel.: +49 30 8104 3137.
E-mail address: juergen.olbricht@rub.de (J. Olbricht).

0925-8388/$ - see front matter © 2013 Elsevier B.V. All rights reserved.
http://dx.doi.org/10.1016/j.jallcom.2013.06.056

The stress-induced transformation to B19′ in NiTi ribbons and wires is well known to occur in a localized (Lüders type) manner [19–27]. Typically, narrow transformation fronts emerge from the grips and move into the gauge length on loading. In displacement controlled tests, these fronts propagate at constant stress until the whole gauge section of the specimen is covered by the transformation, involving a maximum strain of up to 8%, and the situation reverts back on unloading [19–27]. The stress–strain evolution of such a test exhibits characteristic features that are related to the localized type of transformation [19]: (i) a plateau-like constant stress interval is observed in the stress–strain path, both during loading and unloading, for the time period in which the fronts move through the gauge length, and (ii) different sections of the gauge length start to transform (and thus elongate) at distinct points of time. The latter was demonstrated by applying several extensometers during the mechanical test and comparing their reactions on a time scale [19]. A similar analysis of the stress-induced formation of R-phase in a two-extensometer test setup showed that strains of this transformation step were simultaneously evolving in all regions of a pseudoelastic NiTi wire specimen [13], suggesting a homogeneous type of transformation.

Strain measurement methods often overlook detecting the R-phase transformation, as the transformation strains associated to the B2 to R-phase transition are much smaller than those of the B2 to B19′ transformation [15]. Therefore, infrared imaging was used as a complementary method in [13] to prove that non-linearity in the early stress–strain behavior results from transformation events. It was already mentioned there that the obtained temperature profiles suggested homogeneous transformation, and this conclusion was in line with the result of the two-extensometer strain measurements. However, the thermographic analysis in [13] did not cover the whole specimen length and additional experimental verification seemed necessary. The present work aims to further clarify the character of the R-phase transformation by combining mechanical findings with results of an actual thermal imaging analysis.

2. Experimental

Pseudoelastic NiTi wires with a nominal chemical composition of 50.9 at.% Ni were obtained from Memory Metalle, Weil am Rhein, Germany. In the factory, they were hot extruded at 650 °C and wire drawn with 45–55% cold work in the last step. Then, a straight annealing treatment (60 s at 520 °C under a small tensile load) was performed to induce an ultra-fine grained microstructure with optimum pseudoelastic properties. Surface oxides formed during processing were removed by chemical etching. The final wire diameter was 1.2 mm. Further information on the material can be found in [21].

An Instron 5567 electromechanical test machine equipped with a temperature chamber was used for the mechanical characterization of the global pseudoelastic behavior tests reported in this study. Wire specimens with a free gauge length of 40 mm were directly gripped. These tests were carried out at a crosshead displacement rate of 1.67×10^{-3} mm/s (0.1 mm/min) to minimize the effect of the latent heat of transformation. A MTS 632.13F-20 extensometer with 10 mm initial gauge length was attached to the central section of the wire gauge length.

In order to gain further insight into the localized or homogeneous nature of R-phase formation, the surface temperatures of the wire specimens were measured during loading and unloading in a second series of experiments. These experiments were performed in a MTS Bionix 858 servo hydraulic machine. A VarioTHERM infrared imaging system from Infratec, Dresden, Germany was used. The thermal and spatial resolutions of this equipment are better than 0.1 K and 0.2 mm, respectively. Details of the thermal imaging technique were published elsewhere [21,23]. A wire specimen of 35 mm free gauge length was pre-deformed to 0.2 mm. Next, it was elongated from 0.2 mm to 0.354 mm (nominal homogeneous strain: 0.006 to 0.010) at 0.12 mm/s (7 mm/min) crosshead displacement rate, then held for 150 s for thermal equilibrium to be reached. This was followed by unloading to allow contraction of the sample from 0.354 mm to 0.2 mm elongation at similar crosshead displacement rate. After that, the deformation was again kept constant for 150 s to equilibrate temperature with the environment. This cycle was repeated 10 times between the same strain levels of 0.006 and 0.010. Each individual loading or unloading step was completed within 1.32 s and infrared imaging was performed at a frame rate of 1 Hz.

3. Results and discussion

3.1. Mechanically-induced transformations

For the material considered here, stress–strain curves in the range of temperatures between −150 °C and 100 °C have been obtained in a previous study [13] for the assessment of the temperature dependence of stress–strain behavior. At intermediate temperatures, a significant deviation from the initial stress–strain linearity was observed. It was suggested that this effect could be attributed to the stress-induced formation of R-phase. This deviation from linearity is examined more thoroughly in the present work. Fig. 1 illustrates the non-linear behavior at a temperature of 28 °C. The bold line in the figure represents a first cycle in which the wire specimen was only deformed up to the onset of the B19′ transformation plateau and then unloaded. With a sufficiently high resolution (note the expanded strain axis at low strain values), the deviation from linearity and the hysteresis between the loading and unloading branches of the cycle can be clearly appreciated. On complete unloading, no permanent strain is detected, and a second loading (broken line) follows the original load path until the stress level for B19′ formation is reached. In this second cycle, the sample was taken to complete the transformation to B19′. The cycle now exhibits the wide plateaus and hysteresis characteristics of this transformation.

Fig. 2 illustrates how this data can be further analyzed. The first loading/unloading cycle from Fig. 1 is re-plotted here as a solid line and denoted as the original cycle (note the further expanded strain scale compared to Fig. 1). Now, a linear fit to the early deformation range, where the specimen exhibits a basically linear (elastic) behavior, is carried out. Anticipating that this fitted line represents the elastic behavior of the material that could be expected if no phase transformation would occur, the strain deviation of the loading/unloading cycle from this line towards higher stresses can now be determined. Plotting only the strain contribution attributed to R-phase without considering the elastic contribution, the cycle shown in the left part of the diagram is obtained. This stress–strain cycle is characterized by a defined onset of transformation close to 250 MPa and a maximum strain of nearly 0.0035.

An analysis of additional test results in [13] has demonstrated similar reversible non-linear behaviors in temperature range between 28 °C and 42 °C. The non-linearities exhibited a temperature

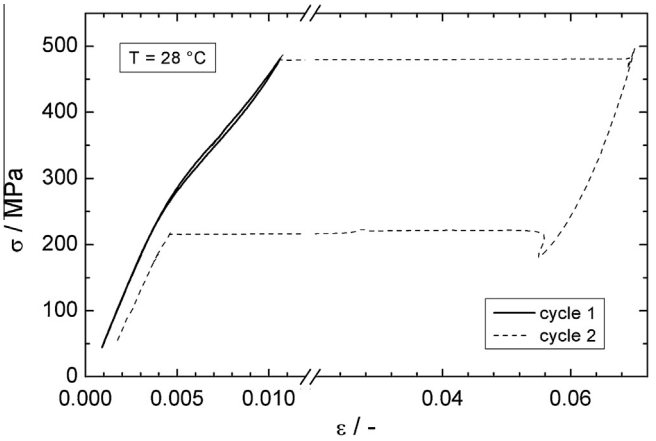

Fig. 1. Two consecutive loading/unloading cycles performed at 28 °C. In the first cycle, the sample is loaded up to the onset of the transformation plateau, and then unloaded. The deviation from linearity and hysteresis in the 275 MPa to 475 MPa stress region is attributed to the transformation to R-phase. The second cycle represents complete transformation to B19′. Note that the strain axis is expanded at low stresses for clarity.

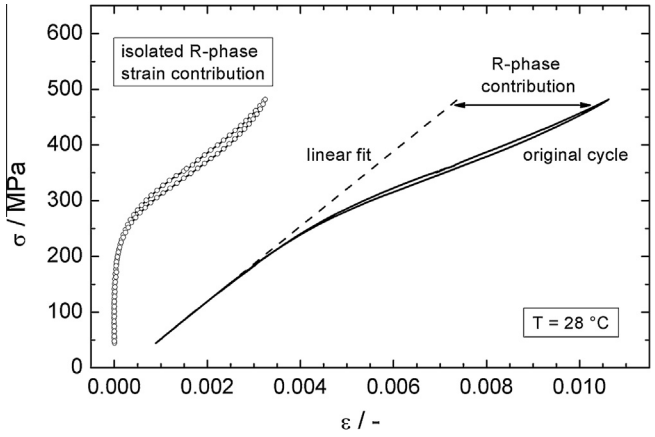

Fig. 2. Analysis of the non-linear stress–strain behavior. The first loading/unloading cycle of Fig. 1 is re-plotted as a solid line (denoted as original cycle). A linear fit to the early elastic behavior at stresses below 125 MPa is plotted as a broken line. The strain resulting from the R-phase transition can be identified as the deviation of the measured cycle from linear behavior. Plotting only this R-phase strain contribution leads to the curve shown on the left.

dependence of (i) the stress levels at which they occurred, and (ii) the amount of strain that was accumulated during R-phase formation. In contrast to the flat, plateau-like load paths of the second cycle in Fig. 1, no periods of constant stress can be detected in Fig. 2 nor in the results in [13] that would indicate a similar heterogeneous Lüders type deformation.

One conceptual limitation of using stress-strain data for assessing the character of the R-phase transformation is related to the fact that the maximum transformation strain expected during this transition is in the range of 1% [15,28]. Small global deformations of this order can easily be overlooked in the analysis of stress–strain data and cannot always be accurately determined due to experimental limitations. Additionally, in the case of a (hypothetical) heterogeneous transition front that encounters an increasing amount of obstacles to advance along its path, a stress-strain curve like the one in the left part of Fig. 2 could also be expected. Infrared thermal imaging was therefore employed as a decisive complementary method to assess the spatial distribution of transformation activity in the specimen. Previous work has shown that R-phase induced specimen temperature variations can be successfully captured by this technique [13].

3.2. Heat effects associated with the formation of R-phase

In Fig. 3, infrared imaging results corresponding to the B2 to R-phase transformation at room temperature are presented. Loading–unloading cycles were applied to a wire specimen following the procedure given in Section 2, resulting in applied stresses of 130 MPa to 315 MPa. This stress range corresponds to the region of non-linear material behavior at this temperature. A high loading rate was applied to establish nearly adiabatic conditions in this experiment, under which the results should be independent of the loading rate. For the last 7 of the 10 performed cycles, the observed final temperature values at the end of the hold periods were the same within the limits of experimental error. These temperature profiles are shown as black curves in Fig. 3; they constitute the reference states for the following loading or unloading action. On applying the strain steps, the corresponding temperature distributions are altered reaching the profiles represented by the lightest grey curves after completing the loading (Fig. 3a) and unloading (Fig. 3b), respectively. Selected additional profiles, at intermediate points of the loading and unloading steps, show how the temperatures evolve in the gauge section of the specimen.

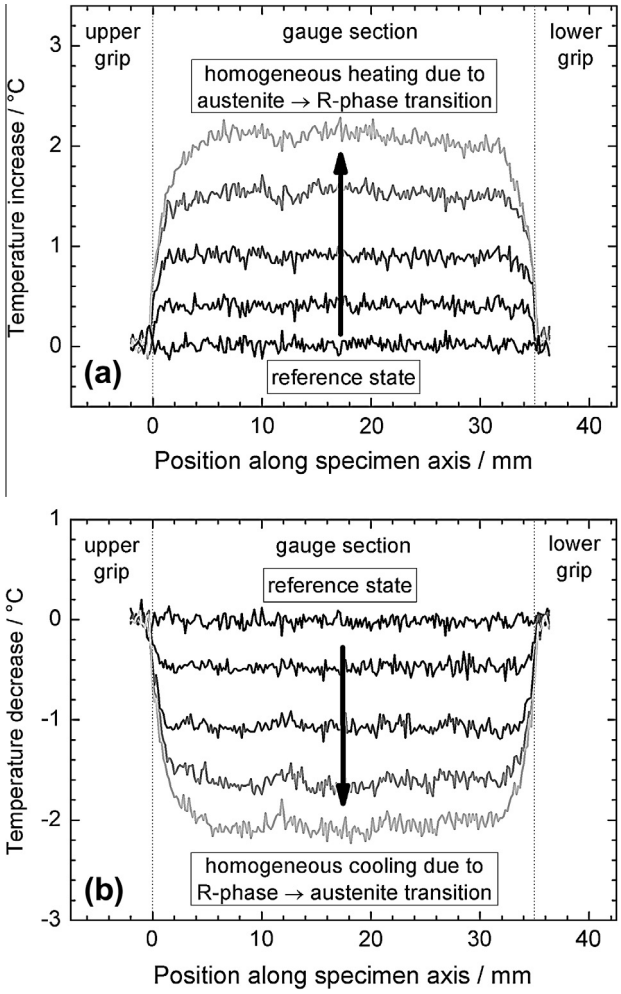

Fig. 3. Infrared thermal imaging results obtained during early deformation of a wire specimen. In both diagrams, the reference profile is shown in black and the final profile in the lightest grey shade. Representative intermediate profiles corresponding to time steps of approximately 0.3 s are also shown. (a) Temperature profiles captured during loading. A homogeneous temperature increase is observed for the central part (from about 5 mm to 30 mm) of the gauge section; (b) temperature distribution during unloading, exhibiting homogeneous cooling effects.

The plotted profiles correspond to time steps of approximately 0.3 s.

The total temperature changes detected in the center of the specimen during loading and unloading are similar within the resolution of the applied method; they slightly exceed a value of 2 °C. In contrast, the specimen grips of the tensile machine represent high thermal masses and, as is apparent from the left and right ends of the profiles in Fig. 3, remain at a constant temperature throughout the experiment. Thus, steep temperature gradients develop in the specimen in the regions close to the grips. The grips act as heat sinks/sources, influencing the temperature profile at the ends of the specimen in a region with a length of about 5 times the wire diameter.

The central part of the specimen (positions between about 5 mm and 30 mm) exhibits the typical temperature effect associated with the transition between B2 and R-phase, i.e., exothermic heat effect during loading and endothermic reaction during unloading, Fig 3. In this region, fully uniform temperature variation is obtained throughout the loading/unloading cycles, which in turn suggests homogeneously distributed transformation activity along the whole gauge section of the specimen. This experimental finding constitutes a definite evidence of the homogeneous nature of

the stress-induced R-phase transformation in ultrafine-grained NiTi.

4. Summary and conclusions

This study has considered a commercially available pseudoelastic NiTi wire with a nominal composition of 50.9 at.% Ni and an ultrafine-grained microstructure formed by wire drawing followed by straight annealing. Precise mechanical experiments and infrared thermal imaging have been used to closely investigate the characteristics of the stress-induced formation of R-phase. The present results allow concluding the following:

(1) The effect of the stress-induced formation of R-phase can be isolated from the overall stress–strain behavior obtained in precise mechanical experiments. Deviations from stress–strain linearity are detected at low applied stresses (below the critical stress for the formation of B19′) which are associated with the stress-induced transformation from B2 to R-phase.
(2) The stress–strain characteristics during the formation of R-phase do not coincide with typical features of the Lüders-type B19′ formation, thus indicating a homogeneous type of transformation.
(3) Thermal imaging reveals that, both during loading and unloading in the range of non-linear stress–strain behavior, homogeneous temperature variations are established in the material. This finding demonstrates that the stress-induced transformation from B2 to R-phase in ultrafine-grained NiTi is a homogeneous process.

Acknowledgements

The authors acknowledge funding by the Deutsche Forschungsgemeinschaft DFG, Land Nordrhein–Westfalen and Ruhr University Bochum through the Collaborative Research Centre on Shape Memory Technology (SFB 459: Formgedächtnistechnik). A.Y. and J.L.P. acknowledge support from CNEA, CONICET, ANPCYT and Univ. Nac. de Cuyo, Argentina.

References

[1] E. Hornbogen, in: W.G.J. Bunk (Ed.), Advanced Structural and Functional Materials, Springer-Verlag, Heidelberg, Germany, 1991, p. 133.
[2] T. Saburi, in: K. Otsuka, C.M. Wayman (Eds.), Shape Memory Materials, Cambridge University Press, Cambridge, UK, 1998, p. 49.
[3] J. Van Humbeeck, Mater. Sci. Eng. A 273–275 (1999) 134.
[4] T. Duerig, A. Pelton, D. Stöckel, Mat. Sci. Eng. A 273–275 (1999) 149.
[5] K. Otsuka, X. Ren, Intermetallics 7 (1999) 511.
[6] T.B. Massalski, H. Okamoto, P.R. Subramanian, L. Kacprzac (Eds.), Binary Alloy Phase Diagrams, vol. 3, second ed., ASM International, OH, 1990, p. 2875.
[7] Y. Kudoh, M. Tokonami, S. Miyazaki, K. Otsuka, Acta Metall. 33 (1985) 2049.
[8] E. Goo, R. Sinclair, Acta Metall. 33 (1985) 1717.
[9] T. Hara, T. Ohba, K. Otsuka, J. Phys. IV 5 (C8) (1996) 641.
[10] J.W. Christian, The Theory of Transformation in Metals and Alloys, third ed., Pergamon Press, Oxford, UK, 2002. pp. 1102.
[11] H. Funakubo, Shape Memory Alloys, Gordon and Breach Science Publishers, New York, 1984.
[12] L. Delaey, in: R.W. Cahn, P. Haasen, E.J. Kramer (Eds.), Phase Transformations in Materials, Materials Science and Technology-Comprehensive Treatment, vol. 5, VCH, Weinheim, 1991, p. 339.
[13] J. Olbricht, A. Yawny, J.L. Pelegrina, A. Dlouhy, G. Eggeler, Met. Mat. Trans. A 42 (2011) 2556.
[14] S. Miyazaki, K. Otsuka, Phil. Mag. 50 (1984) 393.
[15] S. Miyazaki, K. Otsuka, Met. Trans. A 17 (1986) 53.
[16] S. Miyazaki, C.M. Wayman, Acta Met. 36 (1988) 181.
[17] P. Šittner, M. Landa, P. Lukáš, V. Novák, Mech. Matls. 38 (2006) 475.
[18] P. Šittner, P. Sedlák, M. Landa, V. Novák, P. Lukáš, Mat. Sci. Eng. A 438–440 (2006) 579.
[19] S. Miyazaki, T. Imai, K. Otsuka, Y. Suzuki, Scripta Met. 15 (1981) 853.
[20] J.A. Shaw, S. Kyriakides, J. Mech. Phys. Sol. 43 (1995) 1243.
[21] J. Olbricht, Spannungsinduzierte Phasenumwandlungen und funktionelle Ermüdung in ultrafeinkörnigen NiTi-Formgedächtnislegierungen, Shaker Verlag, Aachen, Germany, 2008. pp. 17–95.
[22] J.A. Shaw, S. Kyriakides, Acta Mater. 45 (1997) 683.
[23] S. Gollerthan, M.L. Young, K. Neuking, U. Ramamurty, G. Eggeler, Acta Mat. 57 (2009) 5892.
[24] A. Heckmann, Mikrostruktur und Ermüdung von NiTi-Formgedächtnislegierungen, VDI Verlag, Düsseldorf, Germany, 2003. pp. 81–82.
[25] L.C. Brinson, I. Schmidt, R. Lammering, J. Mech. Phys. Sol. 52 (2004) 1549.
[26] J. Olbricht, A. Schäfer, M.F.-X. Wagner, G. Eggeler, in: S. Miyazaki (Ed.), Proceedings SMST 2007, ASM International, Materials Park, OH, 2007, pp. 47–54.
[27] A. Schäfer, M.F.-X. Wagner, J.L. Pelegrina, J. Olbricht, G. Eggeler, Adv. Eng. Mat. 12 (2010) 453.
[28] G.B. Stachowiak, P.G. McCormick, Acta Met. 36 (1988) 291.